Isochoric *PVTx* Measurements for the C_2H_6 + N_2O Binary System

Francesco Corvaro, Giovanni Di Nicola,* and Marco Pacetti

Dipartimento di Energetica, Università Politecnica delle Marche, Via Brecce Bianche, 60100, Ancona, Italy

Roman Stryjek

Institute of Physical Chemistry, Polish Academy of Sciences, Warsaw, Poland

In the search for fluids potentially suitable for low-temperature refrigeration applications, we have turned our attention to systems consisting of natural fluids, nitrous oxide (N_2O) and ethane (C_2H_6) in particular. Isochoric *PVTx* measurements are reported for nitrous oxide + ethane for both the two-phase and the superheated vapor regions at temperatures ranging from (216 to 358) K and pressures from (494 to 5261) kPa along 11 isochores. The data obtained in the two-phase region were used to derive VLE parameters using a flash method with the Carnahan−Starling−De Santis equation of state (CSD EOS). The dew point was also found for each isochore from the intersection of the *P*−*T* sequences. The dew points were then used to derive VLE parameters from CSD EOS. Results from the superheated region were compared with the predicted from the virial EOS and CSD EOS.

Introduction

One of the chemicals potentially suitable for use in low-temperature refrigeration applications is nitrous oxide, whose critical parameters and saturated pressures are very similar to those of carbon dioxide. The main advantage of nitrous oxide over carbon dioxide lies in its very low melting temperature, whereas its global warming potential (GWP, which is 310) is low, but not low enough to be considered environmentally friendly.

The thermophysical properties of ethane are well-known. Although the ethane + nitrous oxide system has been used as a system for low-temperature refrigeration applications, its thermophysical properties have yet to be thoroughly elucidated. Isochoric measurements were consequently taken, covering temperatures from (216 to 358) K to make up for the lack of VLE and *PVTx* data. A summary of the properties of nitrous oxide, carbon dioxide, and ethane is presented in Table 1. VLE parameters were derived from data in the two-phase region, applying the Carnahan−Starling−De Santis equation of state (CSD EOS),[1] while data obtained from the superheated region were compared with the predictions obtained with the virial equation of state.

Experimental Section

Chemicals. Ethane and nitrous oxide were supplied by Sol SpA. Their purity was checked by gas chromatography, using a thermal conductivity detector, and found to be 99.99 % for both fluids, basing all estimations on an area response.

Apparatus. The new experimental setup is illustrated in Figure 1. The basic experimental setup has already been described elsewhere,[2] so it is only briefly outlined here. The main changes made to the original apparatus[3,4] concerned the twin thermostatic baths (7) filled with different silicone oils (Baysilone M10 and Baysilone M100, Bayer). After charging with the sample mixture, the setup could be operated over two temperature ranges, approximately from (210 to 290) K and from (290 to 360) K, depending on which bath was used. The two silicone oils have different kinematic viscosity values (10 and 100 cSt at room temperature, respectively). The one with lower kinematic viscosity, due to its higher volatility, was applied only for the low-temperature range, while that with a greater viscosity was applied only at high temperatures. The thermostatic baths were easy to move thanks to the new system configuration. The spherical cells and pressure transducer are immersed in one of

* Corresponding author e-mail: anfreddo@univpm.it.

Table 1. Global Warming Potential (GWP), Triple Point Temperature (T_t), Normal Boiling Temperature (T_b), Critical Temperature (T_c), and Critical Pressure (P_c) of the Investigated Fluids

				critical point	
	GWP	T_t/K	T_b/K	T_c/K	P_c/kPa
R170	20	90.35	184.55	305.33	4871
R744A	310	182.33	184.67	309.57	7245
R744	1	216.59	194.75[a]	304.13	7377

[a] Sublimation temperature at atmospheric pressure.

Table 2. Measurements at Bulk Compositions (z_1) for the C_2H_6 (1) + N_2O (2) System over the Temperature Range (ΔT) and Pressure Range (ΔP) with Resultant Dew Temperatures (T_d) and Dew Pressures (P_d)[a]

				N exp. points				
z_1	ΔT/K	ΔP/kPa	*N*/mol	2ph	Vap	tot	T_d/K	P_d/kPa
0.125	216−353	541−3940	0.42784	11	13	24	263.50	2524.3
0.208	218−353	603−3808	0.41356	6	11	17	261.00	2411.4
0.234	218−358	613−4525	0.49524	11	11	22	267.60	2834.5
0.345	217−353	599−3415	0.36583	9	12	21	256.32	2132.1
0.361	217−353	610−4063	0.45046	10	12	22	263.12	2551.5
0.483	220−358	666−3592	0.38211	9	13	22	259.09	2208.0
0.521	216−323	566−5261	0.78153	15	8	23	282.33	3893.2
0.628	217−353	567−3352	0.36250	9	13	22	259.48	2105.9
0.707	224−358	722−4093	0.45871	10	11	21	268.32	2547.7
0.749	218−353	572−3560	0.40631	10	12	22	264.65	2258.9
0.876	217−353	494−3457	0.38433	10	12	22	267.15	2218.0

[a] 2ph and Vap denote data within the VLE boundary and superheated region, respectively.

10.1021/je0503148 CCC: $33.50
Published on Web 11/08/2005

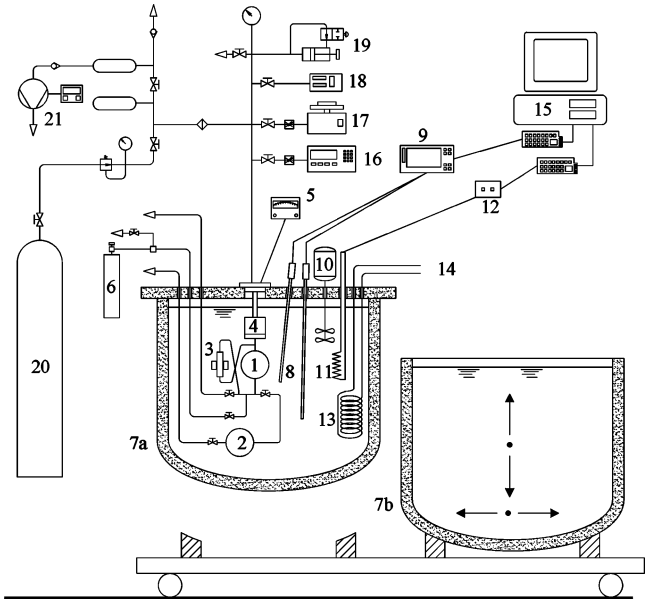

Figure 1. Experimental apparatus: 1, constant volume spherical cell; 2, auxiliary cell; 3, magnetic pump; 4, differential pressure transducer; 5, electronic null indicator; 6, charging system; 7, thermostatic baths; 8, platinum thermoresistances; 9, thermometric bridge; 10, stirrer; 11, heater; 12, power system; 13, cooling coil; 14, connections to auxiliary thermostatic bath; 15, acquisition system; 16, Bourdon gage; 17, dead weight gage; 18, vibrating cylinder; 19, pressure gage; 20, precision pressure controller; 21, nitrogen reservoir; 22, vacuum pump system.

the two thermostatic baths (7). An auxiliary thermostat (14) was used to reach below-ambient temperatures. The cell volume was estimated (as explained elsewhere[4]) to be (273.5 ± 0.3) cm^3 at room temperature.

The pressure and temperature data acquisition systems were identical to those of the previous apparatus.[3,4] A PID device was used to control the temperature, which was measured using a calibrated resistance thermometer; the total uncertainty of the temperature measurements was ± 0.02 K. The uncertainty in the pressure measurements stems from the uncertainty of the transducer and null indicator system and the pressure gauges. The uncertainty of the digital pressure indicator (Ruska, model 7000) is ± 0.003 % of its full scale. Temperature fluctuations due to bath instability can also affect the total uncertainty in the pressure measurement, which was nonetheless found to be less than ± 1 kPa.

Experimental Procedure. Mixtures were prepared using the gravimetric method. First of all, the pure samples were charged in different bottles, degassed to remove noncondensable gases and air, and then weighed with an analytical balance (uncertainty ± 0.3 mg). After evacuating the cell, the bottles were then emptied into the cell immersed in the bath. Then the bottles were weighed again, and the mass of the charge was calculated from the difference between the two masses. The mass of material in the dead volumes was estimated and subtracted from the total mass of the charge. The uncertainty in mixture preparation was estimated to be constantly lower than 0.001 in mole fraction. After reaching the experimental temperature, the mixing pump was activated for about 15 min, and next, the mixture was allowed to stabilize for about 20 min before the data recording.

Results and Discussion

The temperature and pressure ranges are shown in Table 2, along with the mixture's composition and the number of moles charged. On the basis of the analysis of the slope of each $T-P$

Table 3. Experimental Data within the VLE Boundary for the C_2H_6 (1) + N_2O (2) System

T/K	P/kPa	V/dm^3·mol^{-1}	T/K	P/kPa	V/dm^3·mol^{-1}	T/K	P/kPa	V/dm^3·mol^{-1}	T/K	P/kPa	V/dm^3·mol^{-1}
$z_1 = 0.125$						$z_1 = 0.521$					
215.98	541.2	0.637	242.91	1397.9	0.638	215.64	565.9	0.349	252.92	1891.3	0.350
218.13	589.3	0.637	247.89	1628.3	0.638	218.13	621.7	0.349	258.00	2167.0	0.350
223.09	711.5	0.638	252.90	1878.4	0.638	223.08	744.6	0.349	263.05	2469.2	0.350
228.05	851.7	0.638	257.90	2174.1	0.639	228.02	884.4	0.349	268.09	2799.1	0.350
232.95	1010.1	0.638	262.89	2477.6	0.639	232.96	1042.4	0.349	273.07	3154.2	0.350
237.92	1191.9	0.638				237.91	1218.7	0.349	277.87	3528.8	0.350
$z_1 = 0.208$						242.87	1418.5	0.349	282.83	3899.4	0.350
217.73	603.1	0.659	242.92	1434.8	0.660	247.85	1640.6	0.350			
223.08	736.4	0.660	252.88	1928.5	0.660	$z_1 = 0.628$					
232.94	1040.5	0.660	257.98	2221.3	0.661	216.52	567.0	0.752	243.05	1356.1	0.753
$z_1 = 0.234$						223.10	719.4	0.752	248.09	1564.1	0.753
218.03	613.2	0.551	247.98	1678.7	0.551	228.11	852.8	0.753	253.11	1792.4	0.753
223.09	741.3	0.551	252.96	1939.2	0.551	233.08	1012.4	0.753	258.09	2036.2	0.754
228.04	885.6	0.551	258.07	2236.1	0.552	238.07	1170.1	0.753			
232.98	1047.6	0.551	263.05	2555.7	0.552	$z_1 = 0.707$					
237.98	1233.9	0.551	267.98	2834.7	0.552	223.81	721.9	0.595	248.05	1516.1	0.595
243.00	1444.2	0.551				228.12	836.5	0.595	253.04	1736.1	0.595
$z_1 = 0.345$						233.03	973.7	0.595	257.98	1975.4	0.596
216.90	598.8	0.745	243.11	1460.4	0.746	238.07	1136.3	0.595	263.06	2242.6	0.596
223.09	753.8	0.746	248.09	1692.8	0.746	243.04	1315.7	0.595	268.05	2511.2	0.596
228.04	897.4	0.746	253.08	1950.5	0.747	$z_1 = 0.749$					
233.04	1062.7	0.746	258.10	2152.4	0.747	218.14	571.8	0.671	243.11	1280.7	0.672
238.07	1249.6	0.746				223.10	682.0	0.671	249.01	1511.0	0.672
$z_1 = 0.31$						228.08	806.2	0.671	253.10	1687.1	0.672
217.35	609.5	0.605	243.13	1461.2	0.606	233.14	948.5	0.672	258.08	1920.4	0.672
223.13	755.1	0.606	248.12	1693.3	0.606	238.12	1105.7	0.672	263.09	2171.5	0.672
228.12	899.9	0.606	253.11	1951.6	0.606	$z_1 = 0.876$					
233.14	1065.7	0.606	258.10	2236.2	0.606	216.75	494.4	0.709	243.10	1173.7	0.710
238.13	1251.6	0.606	263.09	2534.2	0.607	223.08	621.6	0.710	248.09	1353.0	0.710
$z_1 = 0.483$						228.05	736.1	0.710	253.11	1553.3	0.711
219.89	665.7	0.714	243.09	1433.3	0.714	233.03	864.6	0.710	258.10	1771.3	0.711
223.12	748.6	0.714	248.07	1653.5	0.715	238.10	1011.6	0.710	263.14	2012.6	0.711
228.08	890.4	0.714	253.09	1899.6	0.715						
233.04	1048.7	0.714	258.09	2146.0	0.715						
238.04	1228.5	0.714									

Table 4. Experimental Data in the Superheated Vapor Region for the C_2H_6 (1) + N_2O (2) System

T/K	P/kPa	V/dm^3·mol^{-1}	T/K	P/kPa	V/dm^3·mol^{-1}	T/K	P/kPa	V/dm^3·mol^{-1}	T/K	P/kPa	V/dm^3·mol^{-1}
$z_1 = 0.125$						$z_1 = 0.521$					
267.99	2597.9	0.639	303.09	3173.7	0.640	287.88	4087.0	0.350	307.95	4768.9	0.350
272.97	2682.6	0.639	313.05	3330.4	0.640	293.05	4265.3	0.350	313.04	4936.5	0.351
277.64	2761.6	0.639	323.03	3485.4	0.640	298.08	4437.4	0.350	318.03	5099.4	0.351
283.03	2850.2	0.639	332.99	3638.4	0.641	303.08	4606.1	0.350	323.02	5261.0	0.351
288.01	2931.6	0.639	342.96	3790.3	0.641	$z_1 = 0.628$					
292.99	3012.0	0.639	352.93	3939.7	0.641	263.08	2153.1	0.754	303.07	2704.3	0.755
298.13	3095.1	0.640				268.13	2225.8	0.754	313.04	2836.3	0.755
$z_1 = 0.208$						273.13	2296.2	0.754	323.01	2966.9	0.756
262.97	2439.0	0.661	313.04	3222.9	0.662	278.02	2364.6	0.754	332.99	3096.5	0.756
268.08	2523.7	0.661	322.99	3370.6	0.662	283.02	2433.6	0.754	342.95	3224.6	0.756
273.06	2604.3	0.661	332.97	3517.7	0.663	288.01	2501.8	0.755	352.93	3352.1	0.757
283.02	2763.6	0.661	342.96	3663.8	0.663	292.80	2567.0	0.755			
293.10	2920.5	0.662	352.92	3808.2	0.663	$z_1 = 0.707$					
303.07	3072.8	0.662				272.91	2630.0	0.596	318.08	3425.7	0.597
$z_1 = 0.234$						278.03	2721.9	0.596	327.91	3591.7	0.597
272.92	2937.6	0.552	318.06	3802.1	0.553	283.01	2812.8	0.596	338.09	3762.4	0.598
277.88	3037.0	0.552	328.06	3985.4	0.553	293.08	2992.8	0.596	348.08	3928.3	0.598
282.83	3134.8	0.552	338.10	4166.9	0.554	298.06	3080.5	0.597	358.05	4092.5	0.598
293.11	3334.4	0.552	348.08	4347.0	0.554	308.09	3254.8	0.597			
303.11	3523.6	0.553	358.06	4524.7	0.554	$z_1 = 0.749$					
308.08	3616.8	0.553				268.07	2310.2	0.673	303.07	2845.4	0.674
$z_1 = 0.345$						273.26	2390.0	0.673	313.04	2991.5	0.674
263.09	2225.4	0.747	303.10	2772.2	0.748	278.03	2467.5	0.673	323.01	3136.0	0.674
268.08	2296.2	0.747	313.04	2902.2	0.749	283.01	2544.1	0.673	332.99	3279.3	0.675
273.06	2365.8	0.747	323.02	3032.4	0.749	288.00	2620.0	0.673	342.95	3420.9	0.675
277.87	2431.5	0.747	332.99	3160.9	0.749	298.08	2771.7	0.674	352.87	3560.3	0.675
282.83	2500.7	0.748	342.95	3288.4	0.750	$z_1 = 0.876$					
293.09	2639.1	0.748	352.92	3415.1	0.750	268.14	2219.0	0.711	303.07	2752.3	0.712
$z_1 = 0.361$						273.18	2305.4	0.711	312.98	2895.7	0.713
268.11	2638.4	0.607	303.06	3247.6	0.608	278.02	2381.2	0.711	323.01	3037.9	0.713
273.05	2727.9	0.607	313.04	3414.3	0.608	283.01	2456.7	0.712	332.98	3178.5	0.713
278.03	2816.4	0.607	323.01	3578.5	0.608	288.00	2531.5	0.712	343.07	3319.3	0.713
283.02	2904.0	0.607	332.97	3740.3	0.608	293.09	2606.6	0.712	353.04	3457.3	0.714
288.00	2990.3	0.607	342.95	3902.0	0.609						
293.09	3078.6	0.607	352.92	4062.5	0.609						
$z_1 = 0.483$											
263.02	2263.6	0.715	308.12	2914.0	0.716						
268.11	2340.5	0.715	317.95	3049.9	0.717						
272.92	2412.3	0.715	328.05	3187.9	0.717						
277.86	2485.0	0.716	338.15	3325.0	0.717						
282.84	2557.3	0.716	348.09	3458.9	0.718						
293.12	2703.5	0.716	358.06	3592.0	0.718						
303.04	2842.8	0.716									

sequence, the experimental points were each attributed either to the superheated region or to the two-phase region. Table 3 shows the experimental data within the VLE boundary, while Table 4 contains the *PVTx* data. The number of data belonging to each region is also included in Table 2. The data for the two-phase region were fitted using the Antoine equation, while those relating to the superheated region were fitted by a second-degree polynomial, taking temperature as the independent variable. Then the solution of the two equations representing the system's behavior in the two-phase and superheated regions was used to find the dew point temperature and pressure algebraically for each isochore. The solutions are given in Table 2.

VLE Derivation. Two methods were used to derive VLE data from the isochoric measurements using the CSD EOS, as described elsewhere.[5] This EOS was chosen because, among two-parameters EOSs, it is able to be accurate by representing saturation pressures, volumetric properties along saturation, and vapor phase at superheated region. As it is well-known for all simple EOSs, it is less accurate in the proximity of the critical point, but this region is not touched in the present work.

One method involves deriving the VLE parameters by means of the "dew point" method with the CSD EOS. The dew point parameters (Table 2) were used as independent variables, while the interaction binary parameter (K_{12}) and the corresponding pressure and liquid-phase composition at bubble point (considered as dependent variables) were adjusted to reach the phase equilibrium condition. Table 5 shows the resulting K_{12} values and bubble point parameters. The uncertainty in temperature and pressure of the dew points arising from the data regression with the Antoine and polynomial equations were estimated to be of the order of ± 0.3 K and ± 1 kPa, respectively.

Table 5. Binary Interaction Parameters and Bubble Point Composition (x_1) Found from the Dew Point Applying the CSD EOS

	C_2H_6 (1) + N_2O (2)		
z_1	$K_{12\text{dew}}$	$K_{12\text{flash}}$	x_1
0.125	0.0550	0.0612	0.107
0.208	0.0601	0.0627	0.192
0.234	0.0512	0.0621	0.264
0.345	0.0618	0.0637	0.365
0.361	0.0619	0.0637	0.387
0.483	0.0593	0.0643	0.543
0.521	0.0653	0.0654	0.571
0.628	0.0629	0.0665	0.709
0.707	0.0674	0.0685	0.780
0.749	0.0652	0.0675	0.820
0.876	0.0572	0.0665	0.916
avg	0.0607	0.0648	

The second method involves deriving the VLE parameters for each data point in the two-phase region using the "flash method" with the CSD EOS. For this method to be applied to

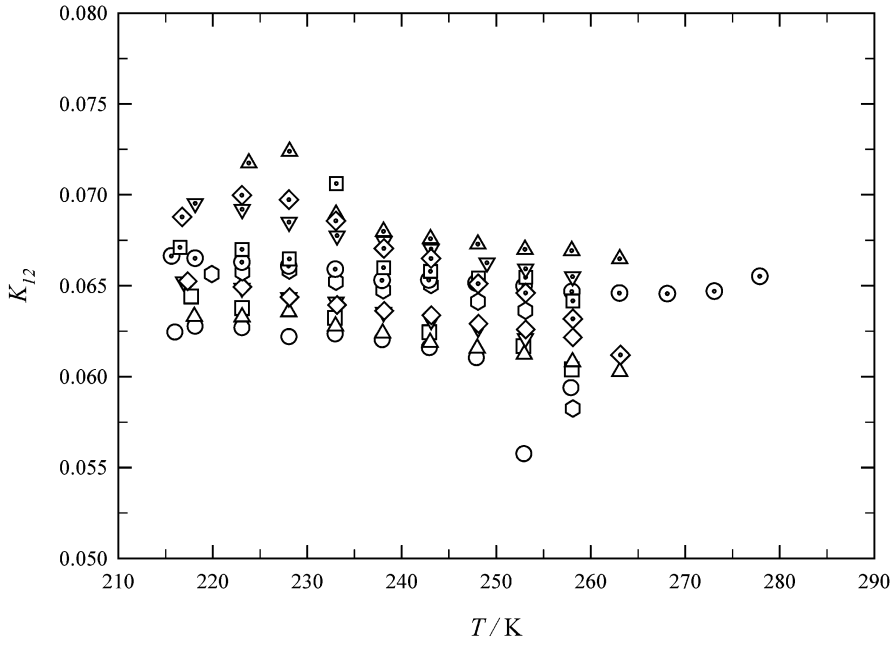

Figure 2. K_{12} values found by the flash method for the C_2H_6 (1) + N_2O (2) system.

○ z_1=0.1248 ▽ z_1=0.3453 ⊙ z_1=0.5208 ⩛ z_1=0.7490
□ z_1=0.2078 ◇ z_1=0.3608 ⊡ z_1=0.6277 ◈ z_1=0.8762
△ z_1=0.2339 ⬡ z_1=0.4827 ⧋ z_1=0.7066

isochoric data, we also need the volumetric properties of both phases, which we calculated from the CSD EOS. T, P, z_i, and n (number of moles charged) were kept constant for each experimental point during the fitting procedure. The isochoric cell volume was known from the gravimetric calibration, so the binary interaction parameter (K_{12}) and the composition at the bubble and dew points were found, considering them as dependent variables. Figure 2 shows the K_{12} values found for each data point in the two-phase region, while Figure 3 shows the scatter diagram of the relative pressure deviations. The behavior of the binary interaction parameters was almost temperature-independent, and the pressure deviations amounted to around ± 1 %.

Using the K_{12} values averaged from our measurements in the two-phase region, we calculated the VLE at three different temperatures. The results are given in Figure 4. Since the properties of N_2O and CO_2 are similar in terms of critical temperature, critical pressure, saturated pressure, and molecular mass, one of our goals was to compare the nitrous oxide and carbon dioxide binary systems. The VLE behavior of C_2H_6 (1)

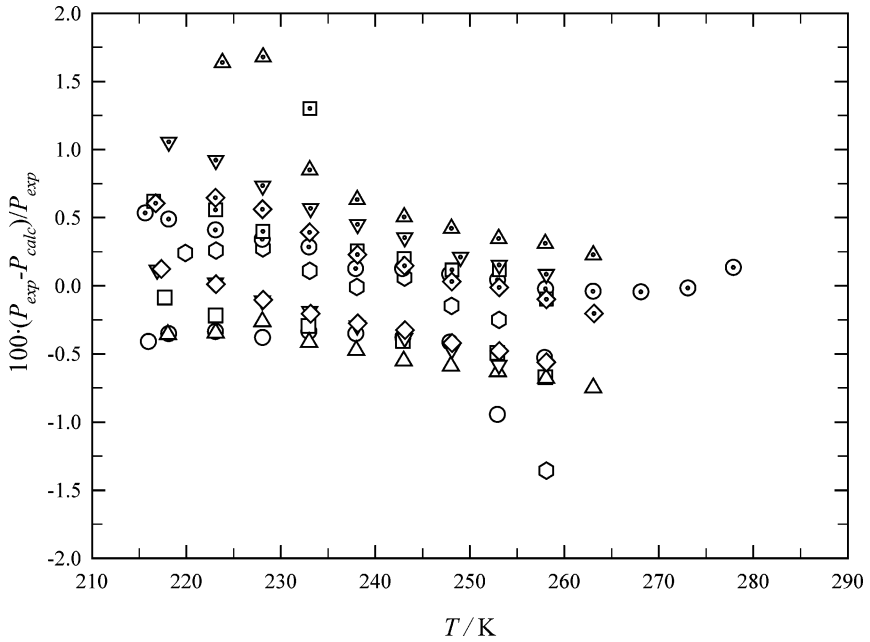

Figure 3. Pressure deviations between experimental values and those calculated with the K_{12} coefficients for the C_2H_6 (1) + N_2O (2) system. Symbols as denoted in Figure 2.

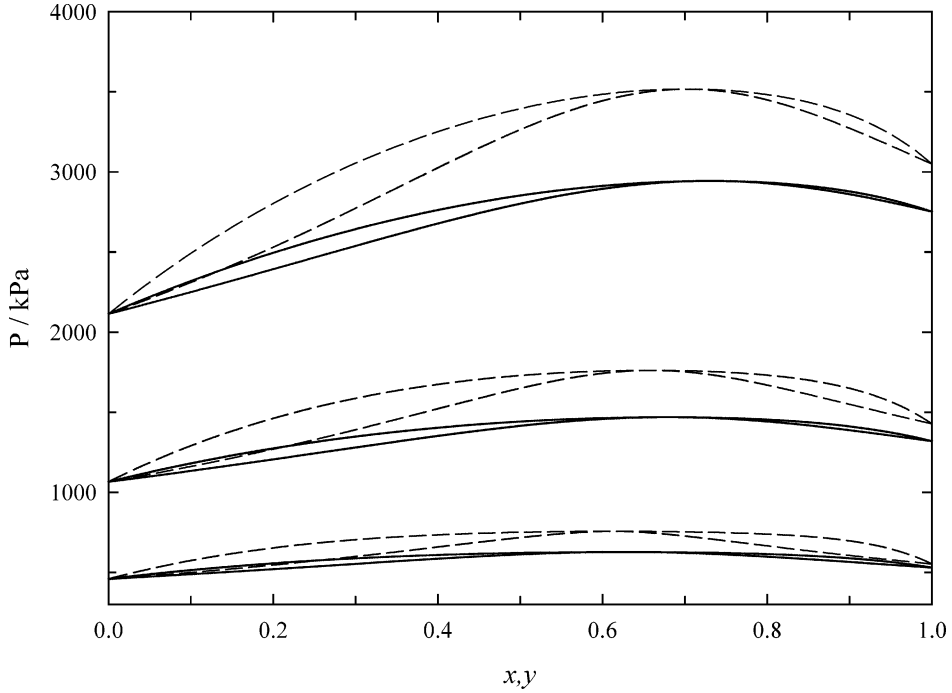

Figure 4. VLE representation from the CSD EOS for the C_2H_6 (1) + N_2O (2) system (solid lines) and for the C_2H_6 (1) + CO_2 (2) system (dashed lines) at three temperatures: $T = 218.15$ K (lowest lines), $T = 243.15$ K (middle lines), and $T = 268.15$ K (upper lines).

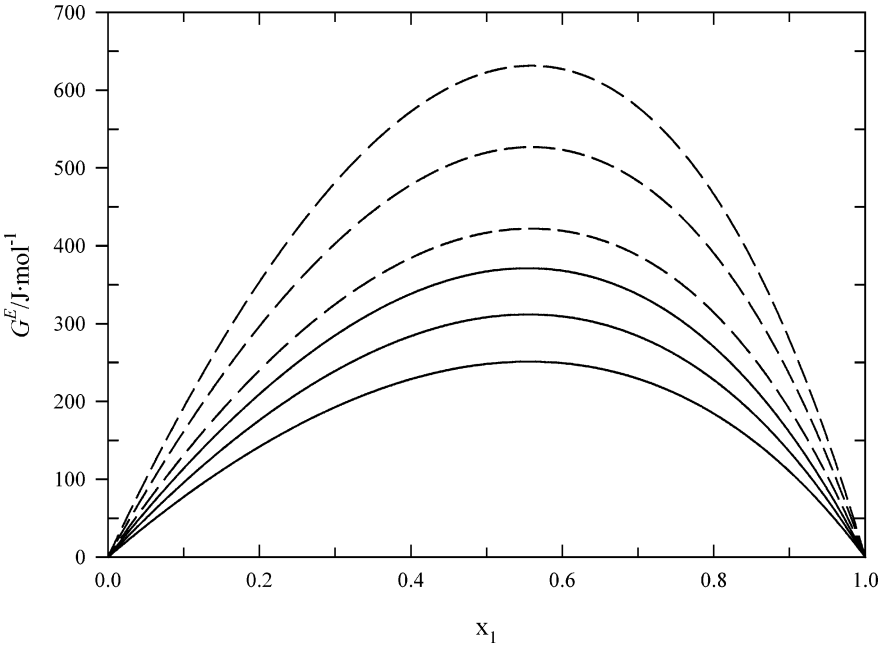

Figure 5. Excess Gibbs energy for the C_2H_6 (1) + N_2O (2) system (solid lines) and for the C_2H_6 (1) + CO_2 (2) system (dashed lines): $T = 218.15$ K (upper lines), $T = 243.15$ K (middle lines), and $T = 268.15$ K (lower lines).

+ CO_2 (2) calculated with the binary interaction parameter (K_{12} = 0.1205) derived from the literature data[6−11] is included in Figure 4 for the comparison.

The C_2H_6 (1) + N_2O (2) system reveals strong positive deviations from Raoult's law, forming a positive azeotrope with an estimated composition around $x_1 = 0.63$, 0.68, and 0.73 at T = (218, 243, and 268) K, respectively. The C_2H_6 + CO_2 system's behavior is qualitatively similar but with distinctly greater deviations from Raoult's law.

The Gibbs excess energy (G^E) calculated using the equation:

$$G^E = RT(\ln \phi - \sum x_i \phi_i) \quad (1)$$

where ϕ and ϕ_i stand for the fugacity coefficients of the mixtures and pure components, respectively, at the same temperature (T) and pressure (P), and R is the gas constant showed a maximum at around $x_1 = 0.55$. The trend of the $G^E(x)$ at the three different temperatures is shown in Figure 5, again for both systems, where the latter's greater deviation from ideality is evident.

PVTx. Since there are no published data on the superheated vapor region for the binary systems considered, we compared our experimental *PVTx* findings with data calculated using the virial EOS in the Leiden form. A temperature dependence of the third-degree polynomial was found for the second and third virial coefficients. Then the pressure values were calculated from the virial equation of state in the Leiden form, using the isochoric experimental temperatures and molar volumes. The

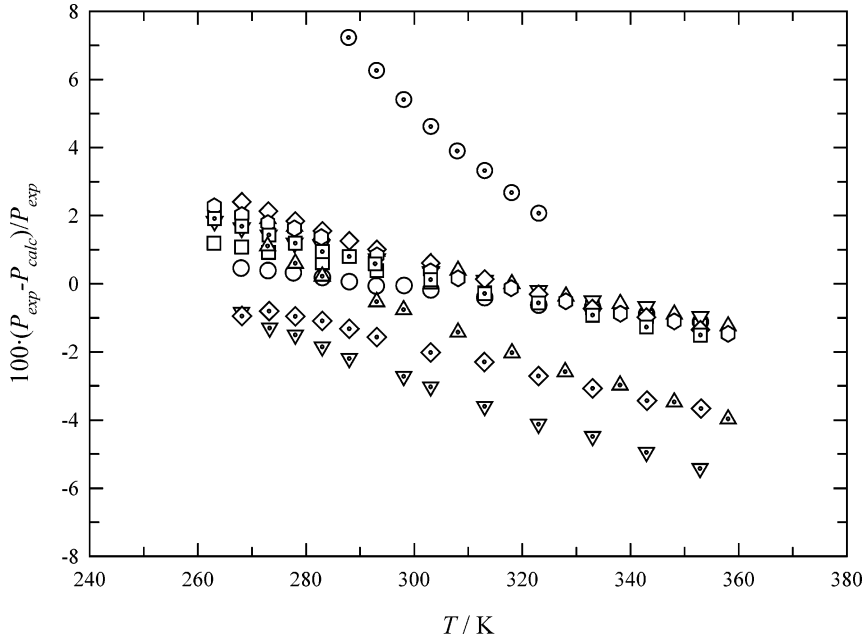

Figure 6. Relative pressure deviations for the C_2H_6 (1) + N_2O (2) system between experimental values from isochoric and data calculated with the virial EOS. Symbols as denoted in Figure 2.

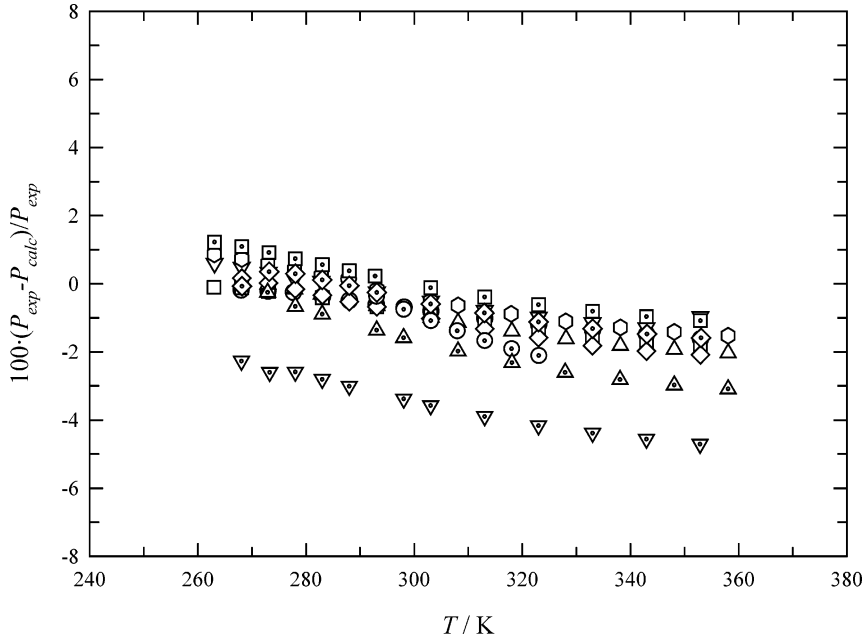

Figure 7. Relative pressure deviations for the C_2H_6 (1) + N_2O (2) system between experimental values from isochoric and data calculated with the CSD EOS. Symbols as denoted in Figure 2.

second and third virial coefficients for the two pure fluids (B_{ii}, B_{jj}, C_{iii}, and C_{jjj}) were drawn from our previous Burnett experiments[12] for nitrous oxide and from the literature[13] for ethane. The following expressions were adopted for the cross virial coefficients (B_{ij}, C_{iij}, and C_{ijj}) because the binary system revealed an almost ideal behavior:

$$B_{ij} = (B_{ii} + B_{jj})/2 \quad (2)$$

$$C_{iij} = (2C_{iii} + C_{jjj})/3 \quad (3)$$

$$C_{ijj} = (C_{iii} + 2C_{jjj})/3 \quad (4)$$

The results are given in Figure 6, showing the relative pressure deviations. Bearing in mind that the comparison is based on cross virial coefficients estimated through eqs 2, 3, and 4 and that the temperature dependence of the virial coefficients was represented by means of third-degree polynomial expressions. The results obtained for one composition ($z_1 = 0.5208$) are clearly out of the deviation trend. For this sample, the mass charged was about twice greater than for all other compositions. In our opinion, the virial equation of state truncated after the third term is not able of accurate representation of the data at greater density. This is why we compared density at superheated region also with the CSD EOS prediction. In this case, the coefficients of the CSD EOS fitted to data along saturation were extrapolated out of range, and also, the K_{12} value, tuned to the low-temperature two-phase data, was assumed to be temperature independent. Deviations between experiments and CSD EOS are presented in Figure 7. The greatest deviation for the sample $z_1 = 0.5208$, observed with the virial EOS prediction, was not

evident when comparing data with the CSD EOS prediction. Moreover, overall deviations in pressures from the CSD EOS prediction showed an AAD = 1.2 %, smaller than the AAD = 1.5 % obtained from the virial EOS comparison. Eventually, it is worth noting that both these models, which are based on different theoretical approaches, showed a similar trend of deviations in terms of temperature.

Conclusions

An isochoric apparatus has been used to obtain *PVTx* measurements on $C_2H_6 + N_2O$. The binary interaction parameters were derived from experimental data in the two-phase region, applying the flash method and the CSD EOS. The dew point parameters were found by interpolating the $P-T$ isochoric sequences, again applying the CSD EOS. The calculated binary interaction parameter were used to derive the VLE, which revealed strong positive deviations from Raoult's law with a positive azeotrope at around $x_1 = 0.65$ and G^E below 300 J/mol at $T = 243.15$ K. The *PVTx* data are consistent with the values predicted by the virial equation of state and the CSD EOS, using its coefficients for the system constituents derived from independent measurements. In general, the *PVTx* are slightly better represented by the CSD EOS.

Literature Cited

(1) De Santis, R.; Gironi, F.; Marrelli, L. Vapor−liquid equilibrium from a hard-sphere equation of state. *Ind. Eng. Chem. Fundam.* **1976**, *15*, 183−189.

(2) Di Nicola, G.; Polonara, F.; Ricci, R.; Stryjek, R. *PVTx* measurements for the R116 + CO_2 and R41 + CO_2 systems. New isochoric apparatus. *J. Chem. Eng. Data* **1995**, *40*, 312−318.

(3) Giuliani, G.; Kumar, S.; Zazzini, P.; Polonara, F. Vapor pressure and gas-phase PVT data and correlation for 1,1,1-trifluoroethane (R143a). *J. Chem. Eng. Data* **1995**, *40*, 903−908.

(4) Giuliani, G.; Kumar, S.; Polonara, F. A constant volume apparatus for vapour pressure and gas phase $P-v-T$ measurements: validation with data for R22 and R134a. *Fluid Phase Equilib.* **1995**, *109*, 265−279.

(5) Di Nicola, G.; Giuliani, G.; Passerini, G.; Polonara, F.; Stryjek, R. Vapor−liquid equilibria (VLE) properties of R-32 + R-134a system derived from isochoric measurements. *Fluid Phase Equilib.* **1998**, *153*, 143−165.

(6) Davalos, J.; Anderson, W. R.; Phelps, R. E.; Kidnay, A. J. Liquid−vapor equilibria at 250.00 K for systems containing methane, ethane and carbon dioxide. *J. Chem. Eng. Data* **1976**, *21*, 81−84.

(7) Gugnoni, R. J.; Eldridge, J. W.; Okay, V. C.; Lee, T J. Carbon dioxide−ethane phase equilibrium and densities from experimental measurements and the B−W−R equation. *AIChE J.* **1974**, *20*, 357−362.

(8) Nagahama, K.; Konishi, H.; Hashino, D.; Hirata, M. Binary vapor-liquid equilibria of carbon dioxide-light hydrocarbons at low temperature. *J. Chem. Eng. Jpn.* **1974**, *7*, 323−328.

(9) Ohgaki, K.; Katayama, T. Isothermal vapor−liquid equilibrium data for the ethane−carbon dioxide system at high pressures. *Fluid Phase Equilib.* **1977**, *1*, 27−32.

(10) Wei, M. S.; Brown, T. S.; Kidnay, A. J.; Dendy Sloan, A. Vapor + liquid equilibria for the ternary system methane + ethane + carbon dioxide at 230 K and its constituent binaries at temperatures from 207 to 270 K. *J. Chem. Eng. Data* **1995**, *40*, 726−731.

(11) Fredenslund A.; Mollerup, J. Measurements and predictions of equilibrium ratios for the $C_2H_6 + CO_2$ system. *J. Chem. Soc., Faraday Trans. 1* **1974**, *70*, 1653−1660.

(12) Di Nicola, G.; Giuliani, G.; Ricci, R.; Stryjek, R. *PVT* properties of dinitrogen monoxide. *J. Chem. Eng. Data* **2004**, *49*, 1465−1468.

(13) Friend, D. G.; Ingham, H.; Ely, J. F. Thermophysical properties of ethane. *J. Phys. Chem. Ref. Data* **1991**, *20*, 275−347.

Received for review August 10, 2005. Accepted October 6, 2005. This work was supported by MIUR, the Ministry of Education, University and Research, and by the Marche Regional Authority.

JE0503148